133

The impact of anodal M1 transcranial direct current stimulation (tDCS) on connectome configuration

Haya Salami[1Ψ], Toni Muffel[2 Ψ], Yvonne Serhan[1], Benjamin Kalloch[2], Uri Hertz[1,4] , Shaymaa Darawshy[1], Arno Villringer[2], Bernhard Sehm[2,3*] , Smadar Ovadia-Caro[1,4*]

Ψ equal contribution, * equal correspondence

1 Department of Cognitive Sciences, University of Haifa, Haifa, Israel
2 Max Planck Institute for Human Cognitive and Brain Sciences, Leipzig, Germany
3 Department of Neurology, University Hospital at the Martine Luther University of Halle-Wittenberg, Halle, Germany
4 The Integrated Brain and Behavior Research Center (IBBRC), University of Haifa, Haifa, Israel

Introduction

- Anodal M1 transcranial direct current stimulation (tDCS) is a common protocol used for enhancing the excitability of the sensorimotor network (SMN) with implementations in both healthy and pathological populations.
- Previous studies have demonstrated changes in functional connectivity within the sensorimotor network as a result of stimulation taking into account small number of regions [1]. However, the impact of stimulation on global connectivity patterns and the network's topology is less well understood.
- Here we aimed at investigating the impact of anodal M1 stimulation on global connectome configuration, and the degree of network segregation.

Methods

Data

16 young healthy participants underwent concurrent MR-tDCS with two conditions per participant: tDCS On (anodal 1mA current over Left M1, cathode over orbitofrontal area for 8.8 minutes), tDCS off (8.8 minutes, electrodes mounted, no current). BOLD fMRI parameters were: 379 Volumes, TR = 1.4 sec, TE =30ms , FOV = 88mm*88mm*64mm.

Pre-processing

Pre-processing was performed using fMRIPrep [2] and complementary in-house scripts using Nilearn [3] tools. Pre-processing included: 4 volumes removal, bandpass filtering (0.01-0.1Hz), and regressing out parameters of motion, white matter, CSF, as well as manually classified noise components. The noise components were generated at the subject level by applying Independent component analysis (ICA). The ICA algorithm implemented by FSL Melodic software [4] decomposed the fMRI data matrix into components each associated with a spatial map and a time course which were later classified as noise or signal components. Noise components were regressed from the data using linear regression.

Analysis

Generalized Canonical Correlation Analysis (GCCA) [5] algorithm was used for linear dimensionality reduction of time-series data coming from all voxels in the grey matter (~20,000). A posteriori parcellation [6] to 7 canonical resting-state networks was applied for post hoc analyses.

Dispersion within networks was calculated as the sum squared of the Euclidean distances from each network node to the network centroid as done in [7] and was calculated at the individual level. Networks centroids were calculated as the median coordinates along the three dimensions at the individual level.

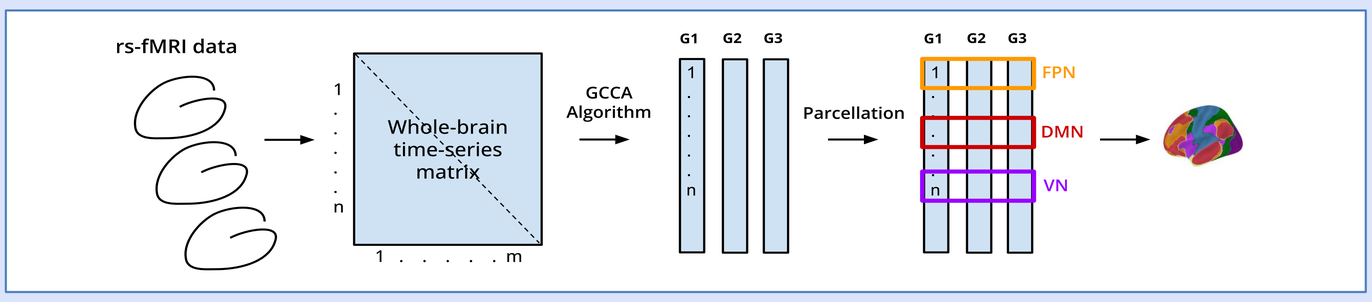

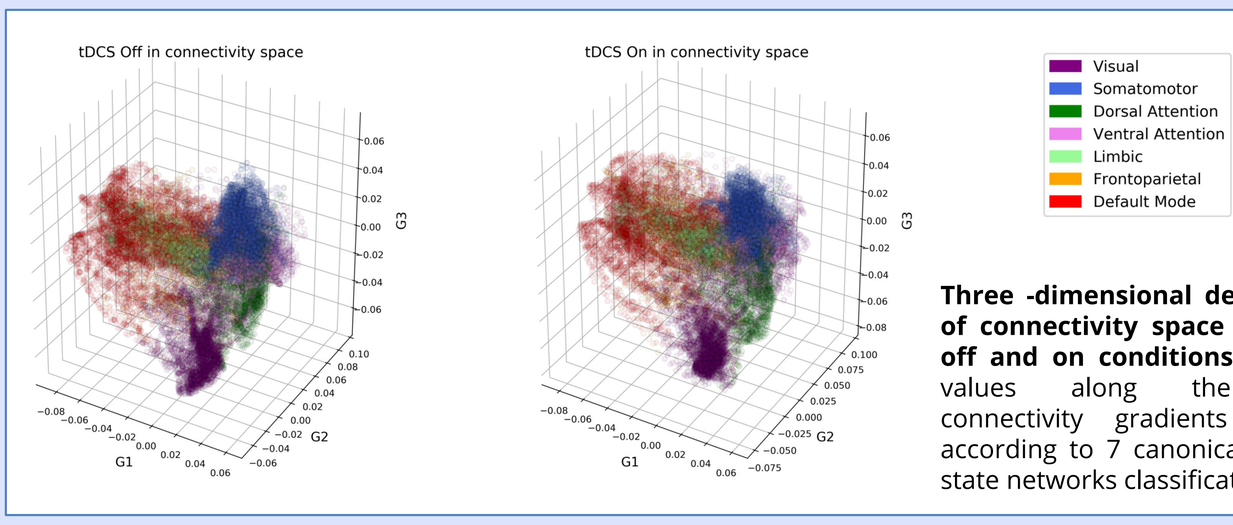

Three -dimensional description of connectivity space for tDCS off and on conditions. Loading values along the three connectivity gradients colored according to 7 canonical resting-state networks classification [6].

Results

1

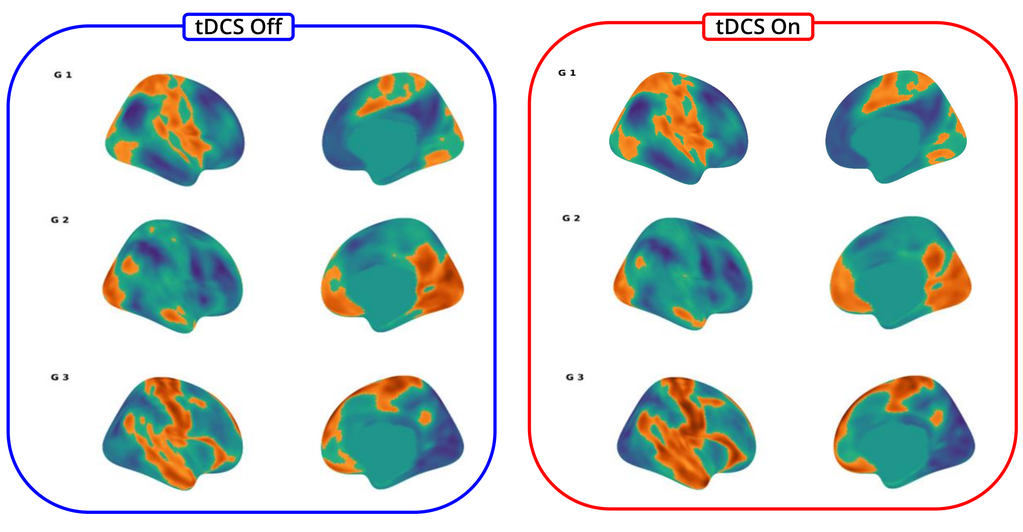

Group-level average gradient maps overlaid on the cortical surface for tDCS off and on conditions. Colors represent loading values for each connectivity gradient (G1, G2, G3). The top row of brain maps shows loading values in tDCS off condition, and the bottom row of brain maps shows loading values of tDCS on condition. All three connectivity gradients do not show an obvious change between the two conditions with respect to the areas implicated on the gradients' two extremes.

2

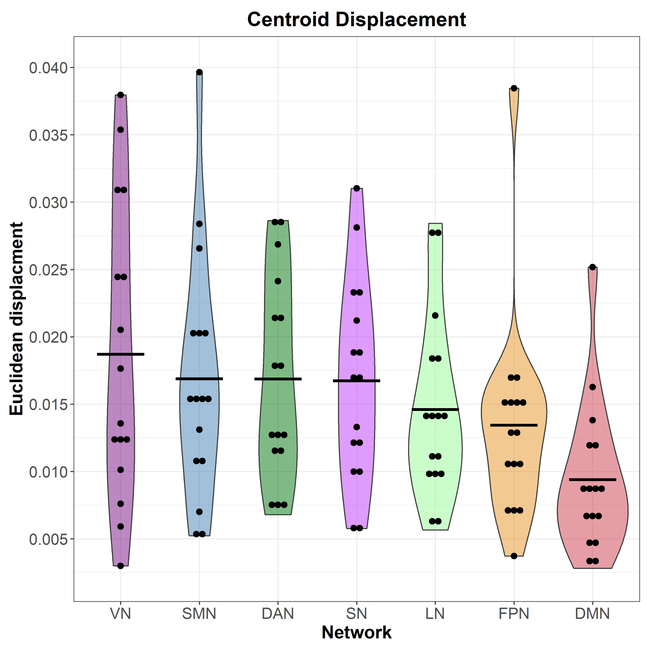

Centroid shifts for tDCS off and on conditions. Network centroids were estimated in 3D gradient space for each subject and the Euclidian distance was calculated between the conditions as a measure of centroid shift. We found global changes in centroid shift, unspecific to the stimulated network. A significant difference in centroid shift was found for the comparison of DMN and the visual network.

Centroid shifts were linearly related to network as a fixed factor Beta ± SE: 0.01688 ± 0.002, t(91) = − 8.43, p < 0.001.

A post hoc Tukey test showed a significant contrast between VN and DMN (t-ratio = 3.58, p-value = 0.009)

3

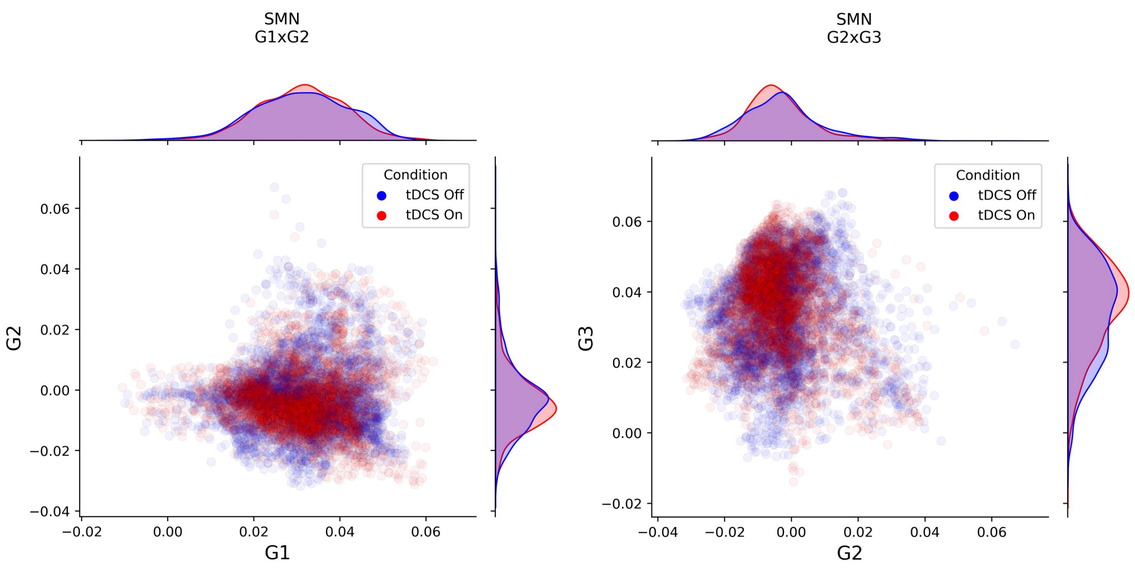

Dispersion changes within SMN as a result of the stimulation. Loading values are plotted for all voxels in SMN network along two dimensions of connectivity gradients. Corresponding density plots are depicted along the respective axes. Descriptively, a decrease in dispersion is visible along all three dimensions in tDCS on condition.

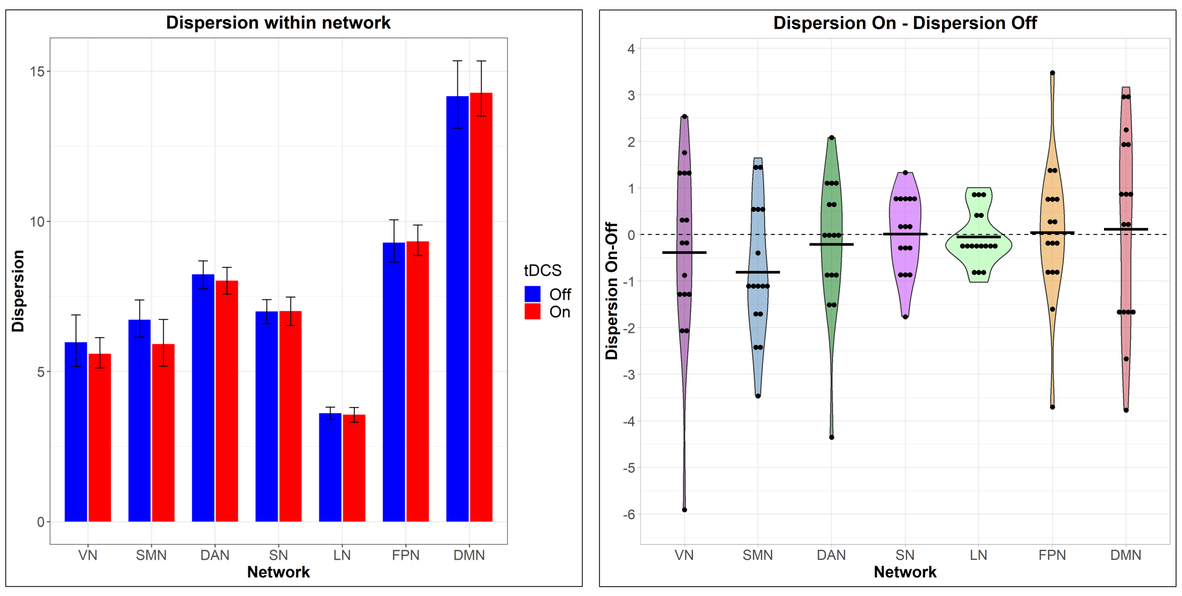

Within network dispersion for tDCS off and on conditions. Dispersion is calculated as the sum of squared Euclidean distances from each network node to the network centroid for each subject. Higher values represent a wider distribution of the network in the 3D gradient space. Dispersion decreased within SMN during tDCS on condition (individual paired t-test, t=2.26, p-value=0.038, uncorrected, Cohen's d=0.57, power calculation with alpha = 0.05 and power of 0.9 yields N=34). On the right, the difference in dispersion values is plotted for individual subjects, and the different networks).

Conclusions

Our results suggest that stimulation of M1 using tDCS has a network-specific effect on sensorimotor networks' dispersion such that the network undergoes segregation in its global connectivity pattern. Networks' centroids on the other hand shift in an unspecific manner, with some networks (DMN) being more stable than others (VN).

References

1. Sehm, B., Kipping, J. A., Schäfer, A., Villringer, A., & Ragert, P. (2013). A comparison between uni-and bilateral tDCS effects on functional connectivity of the human motor cortex. *Frontiers in human neuroscience*, 7, 183.
2. Esteban, O., Markiewicz, C. J., Blair, R. W., Moodie, C. A., Isik, A. I., Erramuzpe, A., Kent, J. D., Goncalves, M., DuPre, E., Snyder, M., Oya, H., Ghosh, S. S., Wright, J., Durnez, J., Poldrack, R. A., & Gorgolewski, K. J. (2018). fMRIPrep: a robust preprocessing pipeline for functional MRI. *Nature Methods*, *16*(1), 111–116.
3. *Nilearn: Statistical Analysis for NeuroImaging in Python — Machine learning for NeuroImaging*. (2010). Nilearn. Retrieved 2022, from https://nilearn.github.io/stable/index.html.
4. Smith, S. M., Jenkinson, M., Woolrich, M. W., Beckmann, C. F., Behrens, T. E., Johansen-Berg, H., Bannister, P. R., de Luca, M., Drobnjak, I., Flitney, D. E., Niazy, R. K., Saunders, J., Vickers, J., Zhang, Y., de Stefano, N., Brady, J. M., & Matthews, P. M. (2004). Advances in functional and structural MR image analysis and implementation as FSL. *NeuroImage*, *23*, S208–S219.
5. KETTENRING, J. R. (1971). Canonical analysis of several sets of variables. *Biometrika*, *58*(3), 433–451.
6. Thomas Yeo, B. T., Krienen, F. M., Sepulcre, J., Sabuncu, M. R., Lashkari, D., Hollinshead, M., Roffman, J. L., Smoller, J. W., Zöllei, L., Polimeni, J. R., Fischl, B., Liu, H., & Buckner, R. L. (2011). The organization of the human cerebral cortex estimated by intrinsic functional connectivity. Journal of Neurophysiology, 106(3), 1125–1165.
7. Bethlehem, R. A., Paquola, C., Seidlitz, J., Ronan, L., Bernhardt, B., Consortium, C. C., & Tsvetanov, K. A. (2020). Dispersion of functional gradients across the adult lifespan. *NeuroImage*, *222*, 117299.